Mineralogical Magazine, August 2016, Vol. 80(5), pp. 855–867

New arsenate minerals from the Arsenatnaya fumarole, Tolbachik volcano, Kamchatka, Russia. VI. Melanarsite, $K_3Cu_7Fe^{3+}O_4(AsO_4)_4$

Igor V. Pekov[1,*], Natalia V. Zubkova[1], Vasiliy O. Yapaskurt[1], Yury S. Polekhovsky[2], Marina F. Vigasina[1], Dmitry I. Belakovskiy[3], Sergey N. Britvin[2,4], Evgeny G. Sidorov[5] and Dmitry Y. Pushcharovsky[1]

[1] Faculty of Geology, Moscow State University, Vorobievy Gory, 119991 Moscow, Russia
[2] St Petersburg State University, Universitetskaya Nab. 7/9, 199034 St Petersburg, Russia
[3] Fersman Mineralogical Museum of the Russian Academy of Sciences, Leninsky Prospekt 18-2, 119071 Moscow, Russia
[4] Nanomaterials Research Center, Kola Science Center of Russian Academy of Sciences, Fersman Str. 18, 184209 Apatity, Russia
[5] Institute of Volcanology and Seismology, Far Eastern Branch of the Russian Academy of Sciences, Piip Boulevard 9, 683006 Petropavlovsk-Kamchatsky, Russia

[*Received 31 May 2015; Accepted 28 August 2015; Associate Editor: G. Diego Gatta*]

ABSTRACT

The new mineral melanarsite, $K_3Cu_7Fe^{3+}O_4(AsO_4)_4$, was found in the sublimates of the Arsenatnaya fumarole at the Second scoria cone of the Northern Breakthrough of the Great Tolbachik Fissure Eruption, Tolbachik volcano, Kamchatka Peninsula, Russia. It is associated with dmisokolovite, shchurovskyite, bradaczekite, hematite, tenorite, aphthitalite, johillerite, arsmirandite, As-bearing orthoclase, hatertite, pharmazincite, etc. Melanarsite occurs as tabular to prismatic crystals up to 0.4 mm, separate or combined in clusters up to 1 mm across or in interrupted crusts up to 0.02 cm × 1 cm × 1 cm covering basalt scoria. The mineral is opaque, black, with a vitreous lustre. Melanarsite is brittle. Mohs' hardness is ~4 and the mean VHN = 203 kg mm^{-2}. Cleavage was not observed and the fracture is uneven. D_{calc} is 4.39 g cm^{-3}. In reflected light, melanarsite is dark grey. Bireflectance is weak, anisotropism is very weak. Reflectance values [R_1–R_2, % (λ, nm)] are 10.5–9.4 (470), 10.0–8.9 (546), 9.7–8.7 (589), 9.5–8.6 (650). The Raman spectrum is reported. Chemical composition (wt.%, electron microprobe) is K_2O 10.70, CaO 0.03, CuO 45.11, ZnO 0.24, Al_2O_3 0.32, Fe_2O_3 6.11, TiO_2 0.12, P_2O_5 0.07, As_2O_5 36.86, total 99.56. The empirical formula, based on 20 O apfu, is $(K_{2.81}Ca_{0.01})_{\Sigma 2.82}(Cu_{7.02}Fe^{3+}_{0.95}Al_{0.08}Zn_{0.04}Ti_{0.02})_{\Sigma 8.11}(As_{3.97}P_{0.01})_{\Sigma 3.98}O_{20}$. Melanarsite is monoclinic, $C2/c$, a = 11.4763(9), b = 16.620(2), c = 10.1322(8) Å, β = 105.078(9)°, V = 1866.0(3) Å^3 and Z = 4. The strongest reflections of the powder X-ray diffraction pattern [d,Å(I)(hkl)] are 9.22(100)(110), 7.59(35)($\bar{1}$11), 6.084(17)(111), 4.595(26)($\bar{1}$31, 220, $\bar{2}$21), 3.124(22)($\bar{3}$31, $\bar{1}$51), 2.763(20)(400, $\bar{1}$52), 2.570(23)(043) and 2.473(16)(260, $\bar{2}$61, 350). Melanarsite has a novel structure type. Its crystal structure, solved from single-crystal X-ray diffraction data (R = 0.091), is based upon a heteropolyhedral pseudo-framework built by distorted Cu(1–3)O_6 and (Fe,Cu)O_6 octahedra and As(1–3)O_4 tetrahedra. Two crystallographically independent K^+ cations are located in the tunnels and voids of the pseudo-framework centring eight- and seven-fold polyhedra. The name reflects the mineral being an arsenate and its black colour (from the Greek μέλαν, black).

Keywords: melanarsite, new mineral, potassium copper iron arsenate, crystal structure, fumarole sublimate, Tolbachik volcano, Kamchatka.

Introduction

This paper continues a series of articles on new arsenates from the Arsenatnaya fumarole located at

*E-mail: igorpekov@mail.ru
DOI: 10.1180/minmag.2016.080.027

© 2016 The Mineralogical Society

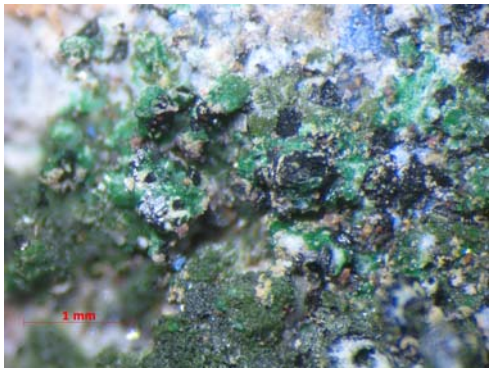

FIG. 1. Black crystals of melanarsite associated with bright green dmisokolovite, olive green shchurovskyite, blue bradaczekite and white As-bearing orthoclase. All these minerals form thin crusts on light-brown basalt scoria altered by fumarolic gas. Field of view: 4.4 mm. Photo: I.V. Pekov and A.V. Kasatkin.

the apical part of the Second scoria cone of the Northern Breakthrough of the Great Tolbachik Fissure Eruption, Tolbachik volcano, Kamchatka Peninsula, Far-Eastern Region, Russia (55°41'N 160°14'E, 1200 m asl). This active, hot fumarole, discovered by us in July 2012, was characterized in the first article of the series devoted to the new mineral yurmarinite $Na_7(Fe^{3+},Mg,Cu)_4(AsO_4)_6$ (Pekov *et al.*, 2014*b*). In subsequent papers we described two polymorphous modifications of $Cu_4O(AsO_4)_2$, ericlaxmanite and kozyrevskite (Pekov *et al.*, 2014*c*), popovite $Cu_5O_2(AsO_4)_2$ (Pekov *et al.*, 2015*b*), structurally related shchurovskyite $K_2CaCu_6O_2(AsO_4)_4$ and dmisokolovite

FIG. 2. Black, coarsely crystalline crust of melanarsite partially overgrown by bright green dmisokolovite. Field of view: 5.9 mm. Photo: I.V. Pekov and A.V. Kasatkin.

$K_3Cu_5AlO_2(AsO_4)_4$ (Pekov *et al.*, 2015*c*) and katiarsite $KTiO(AsO_4)$ (Pekov *et al.*, 2016). In this paper the mineralogical description and crystal structure data for a new mineral melanarsite $K_3Cu_7Fe^{3+}O_4(AsO_4)_4$ (Cyrillic: меланарсит) are given. The name reflects its being an arsenate and its black colour (from the Greek μέλαν, black), very rare for minerals of this chemical class. Both the new mineral and its name have been approved by the IMA Commission on New Minerals, Nomenclature and Classification (MA2014–048, Pekov *et al.*, 2014*e*). The type specimen is deposited in the systematic collection of the Fersman Mineralogical Museum of the Russian Academy of Sciences, Moscow, catalogue number 94992.

Occurrence and general appearance

Specimens with melanarsite were collected by us in July 2013 in the southern part of the Arsenatnaya fumarole, at a depth ~0.5 m below the surface. The temperature measured using a chromel-alumel thermocouple immediately after uncovering the mineralized pockets was 360–380°C. Melanarsite was found in incrustations mainly consisting of arsenates, oxides and sulfates. We believe that the new mineral was deposited directly from the gas phase as a volcanic sublimate at temperatures not lower than 380°C (see Discussion).

Melanarsite occurs as well-shaped or, more commonly, coarse crystals up to 0.1 mm, rarely up to 0.4 mm in size, separate or combined in dense or open-work clusters up to 1 mm across, rarely forming interrupted incrustations up to 1 cm × 1 cm in area and up to 0.2 mm thick covering basalt scoria (Figs 1 to 3). Melanarsite crystals are tabular to prismatic, typically angled obliquely (Fig. 3). Usually they have a skeletal and/or blocky character. Their parallel or near-parallel intergrowths are sometimes combined in crusts (Fig. 3*c*,*d*). The most typical minerals associated intimately with melanarsite are dmisokolovite, shchurovskyite, bradaczekite $NaCu_4(AsO_4)_3$, hematite, As-bearing orthoclase (Figs 1, 2, 4 and 5), johillerite $Na(Mg,Cu)_3Cu(AsO_4)_3$, arsmirandite $Na_{18}Cu_{12}Fe^{3+}O_8(AsO_4)_8Cl_5$ (IMA2014–081, Pekov *et al.*, 2015*a*), aphthitalite, tenorite, langbeinite, anhydrite, tilasite and fluorophlogopite. In some cases the new mineral is associated closely with hatertite $Na_2(Ca,Na)(Fe^{3+},Cu)_2(AsO_4)_3$ (Fig. 4) or pharmazincite $KZnAsO_4$ (IMA2014-015, Pekov *et al.*, 2014*a*) (Fig. 5).

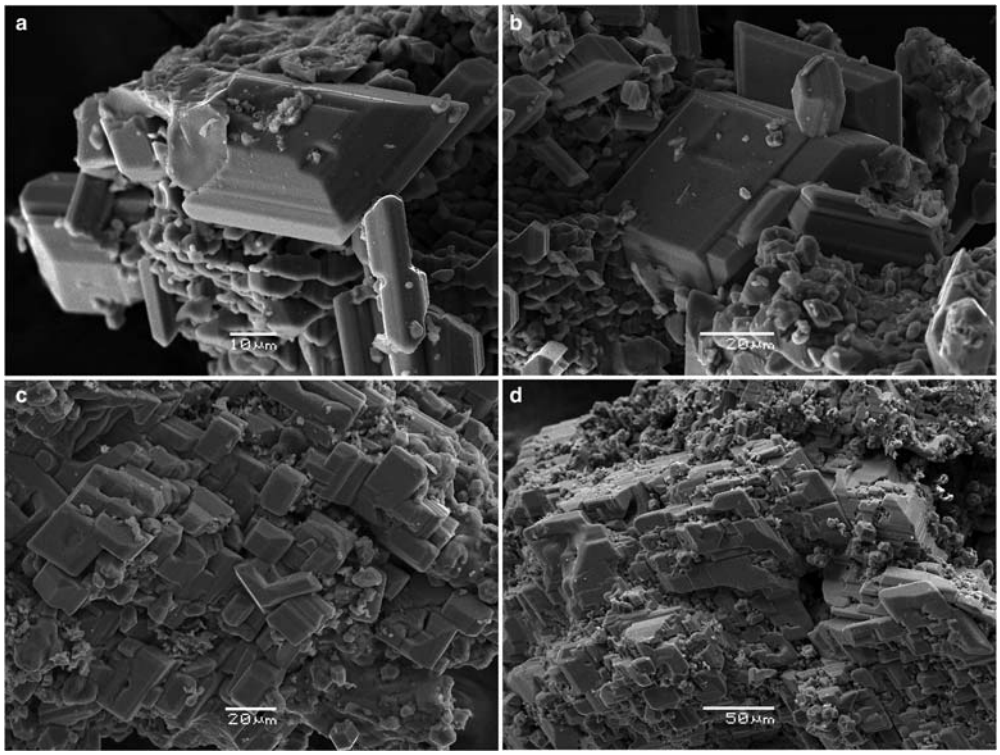

FIG. 3. Well-shaped crystals (*a*, *b*) and crystal crusts (*c*, *d*) of melanarsite. Scanning electron microscopy (SEM) secondary electron image.

Physical properties and optical data

Melanarsite is black, with a strong vitreous lustre. It is megascopically opaque; only very thin sections are translucent and dark green. Its streak is dark green with an olive hue. The mineral is brittle. Cleavage or parting is not observed. The fracture is uneven. Mohs hardness is ~4. The mean micro-indentation hardness (VHN) is 203, range 178–225 kg mm^{-2} (load 10 g). Density could not

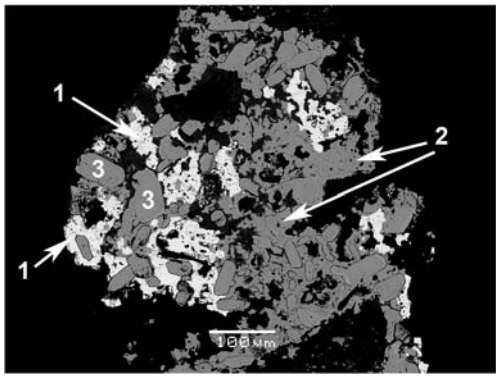

FIG. 4. Aggregates of melanarsite (1) and hatertite (2) overgrowing well-shaped crystals of hematite (3). Polished section. SEM back-scatter electron image.

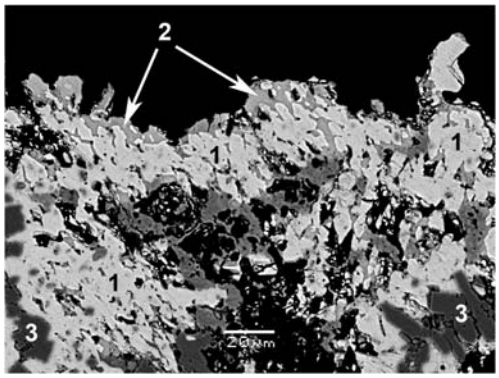

FIG. 5. Crystal crust composed by (1) melanarsite, (2) pharmazincite $KZnAsO_4$ (IMA2014-015) and (3) hematite. Polished section. SEM back-scatter electron image.

TABLE 1. Reflectance data for melanarsite*.

λ, nm	R_1, %	R_2, %	λ, nm	R_1, %	R_2, %
400	11.4	10.2	560	9.9	8.8
420	11.1	9.9	580	9.8	8.7
440	10.9	9.7	**589**	**9.7**	**8.7**
460	10.6	9.4	600	9.7	8.7
470	**10.5**	**9.4**	620	9.6	8.6
480	10.4	9.3	640	9.5	8.6
500	10.2	9.1	**650**	**9.5**	**8.6**
520	10.1	9.0	660	9.4	8.5
540	10.0	8.9	680	9.4	8.4
546	**10.0**	**8.9**	700	9.3	8.4

*Values for wavenumbers (λ) recommended by the Commission on Ore Mineralogy (COM) are given in bold.

be measured because monomineralic, massive (without caverns or inclusions) particles of melanarsite are too small for volumetric methods and because of a lack of heavy liquids of necessary density. Density calculated using its empirical formula is 4.386 g cm^{-3}.

Under the microscope in reflected light, melanarsite is dark grey and pleochroism was not observed. Bireflectance is weak, $\Delta R = 1.0\%$ (589 nm). Anisotropism is very weak. The reflectance values measured by a MSF-21 microspectrophotometer (LOMO, Russia) using SiC standard (Zeiss, No. 545) are given in Table 1. Under the microscope in transmitted light, melanarsite particles larger than 5–7 μm are not transparent and optical data can be obtained only for tiny particles (3–5 μm). Because of this and the high refractivity of the mineral, the data are of poor quality. Melanarsite is biaxial, $\alpha = 1.80(1)$, β was not measured and $\gamma = 1.91(1)$. Optical sign and 2V were not determined. Dispersion was not observed. Pleochroism, observed in the thinnest particles, is strong with *Z* (very dark greyish-green) > *X* (green to pale green).

Raman spectroscopy

The Raman spectrum of melanarsite (Fig. 6) was recorded for a randomly orientated crystal using an EnSpectr R532 instrument (Department of Mineralogy, Moscow State University) with a green laser (532 nm) at room temperature. The output power of the laser beam was ~4 mW. The spectrum was processed using the EnSpectr expert mode program in the range 100 to 4000 cm^{-1} with a holographic diffraction grating with 1800 lines cm^{-1} and a resolution of 5–8 cm^{-1}. The diameter of the focal spot on the sample was ~15 μm. The back-scattered Raman signal was collected with 40x objective; signal acquisition time for a single scan of the wavelength range was 1500 ms and the signal was averaged over 10 scans. Two strong bands in the range 770 to 870 cm^{-1} correspond to As^{5+}–O stretching vibrations of AsO_4^{3-} anions. Bands with frequencies lower than 650 cm^{-1} correspond to bending vibrations in AsO_4 tetrahedra, Cu^{2+}–O stretching vibrations and lattice modes. In particular,

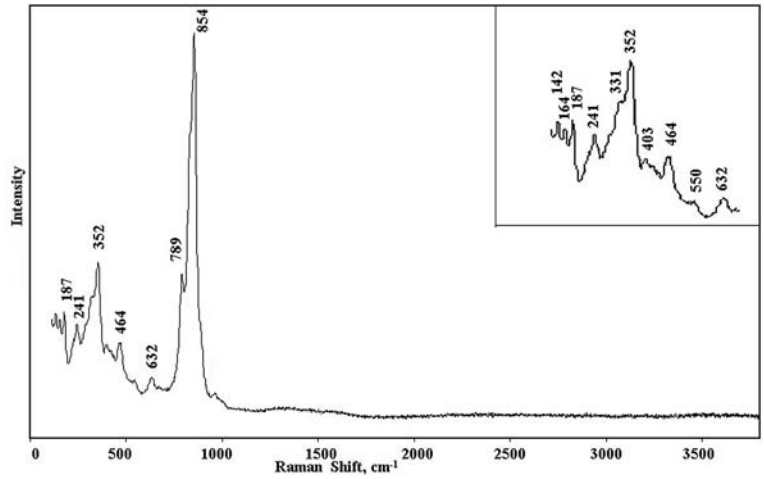

FIG. 6. Raman spectrum of melanarsite with an enlarged section showing the low-frequency region.

TABLE 2. Powder X-ray diffraction data for melanarsite.

I_{obs}	d_{obs}	I_{calc}*	d_{calc}**	*h k l*
100	9.22	100	9.220	110
35	7.59	42	7.578	$\bar{1}11$
17	6.084	20	6.085	111
4	4.958	4	4.955	130
6	4.905	4	4.892	002
7	4.779	8	4.770	$\bar{1}12$
26	4.595	4, 14, 9	4.644, 4.610, 4.569	$\bar{1}31$, 220, $\bar{2}21$
6	4.251	3	4.257	$\bar{2}02$
4	4.222	1, 3	4.227, 4.216	131, 022
14	3.979	6	3.979	112
12	3.826	9, 2	3.826, 3.824	221, 041
12	3.686	5	3.703	$\bar{1}32$
3	3.337	1	3.335	$\bar{3}12$
5	3.331	1	3.324	240
8	3.289	11, 3	3.295, 3.269	132, 202
22	3.124	1, 15, 8	3.135, 3.132, 3.096	311, $\bar{3}31$, $\bar{1}51$
8	3.078	10	3.073	330
14	3.038	23, 3	3.042, 3.036	222, 023
14	2.990	24	2.984	$\bar{2}23$
14	2.966	30	2.963	151
5	2.887	10	2.882	$\bar{1}33$
6	2.797	14	2.798	$\bar{3}13$
20	2.763	23, 1, 9	2.770, 2.766, 2.765	400, 331, $\bar{1}52$
11	2.739	18	2.735	$\bar{4}02$
14	2.599	36, 2, 9	2.604, 2.598, 2.589	312, $\bar{4}22$, 133
23	2.570	35	2.565	043
14	2.503	1, 22, 1	2.502, 2.501, 2.490	$\bar{1}14$, $\bar{3}51$, $\bar{2}04$
16	2.473	7, 14, 6	2.478, 2.471, 2.471	260, $\bar{2}61$, 350
2	2.433	3	2.426	223
2	2.408	2	2.410	062
7	2.317	1, 24	2.322, 2.316	$\bar{2}62$, $\bar{3}14$
6	2.176	12	2.180	402
9	2.130	12	2.129	$\bar{4}04$
5	2.113	1, 1, 10, 1	2.119, 2.111, 2.110, 2.098	$\bar{5}31$, 063, $\bar{4}43$, 134
9	2.077	14	2.078	080
2	2.055	3, 1	2.058, 2.054	530, 172
1	2.015	1	2.014	$\bar{1}54$
1	1.968	1	1.968	$\bar{5}33$
1	1.946	1, 1, 1	1.947, 1.945, 1.942	$\bar{3}72$, 280, $\bar{2}81$
1	1.897	2, 1	1.899, 1.897	$\bar{6}02$, $\bar{1}35$
2	1.868	2, 1, 1	1.873, 1.871, 1.864	154, 263, $\bar{5}52$
7	1.842	1, 1, 1	1.847, 1.844, 1.844	600, 173, 550
3	1.821	2, 2, 1	1.823, 1.822, 1.821	353, 190, 314
4	1.803	5, 3	1.805, 1.803	$\bar{1}91$, 620
3	1.783	3	1.781	$\bar{6}23$
3	1.779	1, 4	1.779, 1.777	$\bar{5}53$, 191
1	1.751	1	1.752	135
2	1.731	1, 2, 3, 3	1.734, 1.732, 1.731, 1.726	$\bar{6}41$, $\bar{1}74$, $\bar{1}92$, $\bar{1}55$
3	1.716	11	1.715	443
3	1.685	2, 8	1.684, 1.682	192, $\bar{4}45$
4	1.659	4, 1, 3	1.662, 1.662, 1.654	480, 0.10.0, $\bar{4}82$
6	1.632	3, 1, 16, 2, 2	1.635, 1.633, 1.631, 1.628, 1.628	404, $\bar{5}72$, 006, $\bar{7}12$, $\bar{5}35$

(continued)

TABLE 2. (*contd.*)

I_{obs}	d_{obs}	I_{calc}*	d_{calc}**	*h k l*
3	1.621	1, 1, 2	1.623, 1.623, 1.620	$\bar{7}11$, $\bar{3}92$, 570
4	1.599	2, 3, 1, 1, 2	1.601, 1.599, 1.598, 1.598, 1.598	641, $\bar{4}06$, 391, 065, 481
3	1.592	2, 2, 1, 1	1.592, 1.590, 1.590, 1.589	2.10.0, $\bar{2}$.10.1, $\bar{3}36$, $\bar{7}13$
3	1.576	3, 1	1.576, 1.574	710, 0.10.2
2	1.561	2	1.565	$\bar{7}31$
3	1.513	4, 11, 2	1.515, 1.513, 1.509	$\bar{7}14$, 392, 335
6	1.488	2, 1, 6, 2, 2	1.492, 1.488, 1.487, 1.487, 1.485	$\bar{1}94$, $\bar{1}$.11.1, $\bar{5}74$, $\bar{4}84$, $\bar{3}56$
1	1.476	3, 2	1.475, 1.474	$\bar{2}$.10.3, 553

*For the calculated pattern, only reflections with intensities ≥1 are given. **For unit-cell parameters calculated from single-crystal data.

the band at 632 cm^{-1} can be assigned as a Cu–O stretching mode and the strong band at 352 cm^{-1} as an O–As–O bending mode. The absence of bands with frequencies higher than 1000 cm^{-1} indicates the absence of groups with O–H, C–H, C–O, N–H, N–O and B–O bonds in the mineral.

Chemical composition

The chemical composition of melanarsite was studied using a Jeol JSM-6480LV scanning electron microscope equipped with an INCA-Wave 500 wavelength-dispersive spectrometer (Laboratory of

TABLE 3. Crystal data, data collection information and structure refinement details for melanarsite.

Formula	$K_3Cu_7Fe(AsO_4)_4O_4$
Formula weight	1237.61
Temperature, K	293(2)
Radiation and wavelength, Å	Mo*K*α; 0.71073
Crystal system, space group, *Z*	Monoclinic, *C*2/c; 4
Unit-cell dimensions, Å, °	*a* = 11.4763(9) *b* = 16.620(2) β = 105.078(9) *c* = 10.1322(8)
V, Å^3	1866.0(3)
Absorption coefficient μ, mm^{-1}	16.384
F_{000}	2312
Crystal size, mm	0.03 × 0.05 × 0.06
Diffractometer	Xcalibur S CCD
θ range for data collection, °	2.69–26.37
Index ranges	$-14 \le h \le 14$, $-20 \le k \le 20$, $-12 \le l \le 12$
Reflections collected	14,009
Independent reflections	1918 (R_{int} = 0.1256)
Independent reflections with $I > 2\sigma(I)$	1652
Structure solution	direct methods
Refinement method	full-matrix least-squares on F^2
Number of refined parameters	160
Final *R* indices [$I > 2\sigma(I)$]	*R*1 = 0.0914, *wR*2 = 0.1746
R indices (all data)	*R*1 = 0.1095, *wR*2 = 0.1823
Goof	1.278
Largest diff. peak and hole, *e* Å^{-3}	2.355 and –1.569

TABLE 4. Atom coordinates, equivalent isotropic displacement parameters ($Å^2$) and site multiplicities (Q) for melanarsite.

Atom	x/a	y/b	z/c	U_{eq}	Q
As(1)	0.5	0.65808(14)	0.75	0.0106(5)	4
As(2)	0.5	0.77774(14)	0.25	0.0121(6)	4
As(3)	0.79713(15)	0.56128(10)	0.24785(17)	0.0096(4)	8
$(Fe_{0.5}Cu_{0.5})$*	0.9638(2)	0.66941(14)	0.0859(2)	0.0143(6)	8
Cu(1)	0.45787(19)	0.95338(12)	0.0939(2)	0.0111(5)	8
Cu(2)	0.76820(18)	0.42242(12)	0.4141(2)	0.0105(5)	8
Cu(3)	0.69130(17)	0.70371(12)	0.0866(2)	0.0091(5)	8
K(1)	0.5	0.4451(4)	0.75	0.0347(17)	4
K(2)	0.2957(4)	0.3422(4)	0.4385(6)	0.0405(13)	8
O(1)	0.8811(11)	0.9024(7)	0.2321(13)	0.016(3)	8
O(2)	0.6378(12)	0.0269(7)	0.7750(13)	0.018(3)	8
O(3)	0.7452(11)	0.5435(7)	0.3863(13)	0.018(3)	8
O(4)	0.3845(13)	0.2805(8)	0.7594(15)	0.028(3)	8
O(5)	0.8846(12)	0.6440(8)	0.2740(17)	0.031(4)	8
O(6)	0.9493(12)	0.6662(8)	0.6054(14)	0.023(3)	8
O(7)	0.9369(10)	0.5613(7)	0.0250(11)	0.011(2)	8
O(8)	0.8151(10)	0.9149(6)	0.8902(12)	0.011(2)	8
O(9)	–0.0094(11)	0.7844(7)	0.1091(12)	0.013(3)	8
O(10)	0.6970(10)	0.8140(7)	0.0296(11)	0.010(2)	8

*The site content was refined and fixed in the last stages of the refinement.

local methods of matter investigation, Faculty of Geology, Moscow State University), with an acceleration voltage of 20 kV, a beam current of 20 nA and a 3 μm beam diameter. The following standards were used: orthoclase (K), $CaWO_4$ (Ca), $CuFeS_2$ (Fe), ZnS (Zn), Al_2O_3 (Al), ilmenite (Ti), GaP (P) and FeAsS (As). The average (seven spot analyses) chemical composition of melanarsite (wt.%, ranges are in parentheses) is K_2O 10.70 (10.40–10.91), CaO 0.03 (0.00–0.10), CuO 45.11 (44.51–46.25), ZnO 0.24 (0.00–0.55), Al_2O_3 0.32 (0.00–1.36), Fe_2O_3 6.11 (5.49–7.07), TiO_2 0.12 (0.00–0.47), P_2O_5 0.07 (0.00–0.25), As_2O_5 36.86 (35.94–37.77), total 99.56. Contents of other elements with atomic numbers higher than carbon are below detection limits. Fe is considered as Fe^{3+} based on the structure data (see below) and taking into account the extremely oxidizing conditions of mineral deposition in the Arsenatnaya fumarole; all other known iron minerals from the locality contain only Fe^{3+} (Pekov *et al.*, 2014*b*, 2015*c*). The empirical formula of melanarsite, calculated based on 20 O apfu, is $(K_{2.81}Ca_{0.01})_{\Sigma 2.82}(Cu_{7.02}Fe^{3+}_{0.95}Al_{0.08}Zn_{0.04}Ti_{0.02})_{\Sigma 8.11}(As_{3.97}P_{0.01})_{\Sigma 3.98}O_{20}$. The simplified formula is $K_3Cu_7Fe^{3+}O_4(AsO_4)_4$, which requires K_2O 11.42, CuO 44.99, Fe_2O_3 6.45, As_2O_5 37.14, total 100.00 wt.%.

X-ray crystallography

Powder X-ray diffraction data of melanarsite (Table 2) were collected with a Rigaku R-AXIS Rapid II single-crystal diffractometer equipped with a cylindrical image plate detector using Debye-Scherrer geometry (d = 127.4 mm; Co$K\alpha$ radiation). Parameters of the monoclinic unit cell calculated from the powder data are a = 11.460(8), b = 16.630(6), c = 10.146(8) Å, β = 105.21(5)° and V = 1866(3) $Å^3$.

Single-crystal X-ray studies of melanarsite were carried out using an Xcalibur S diffractometer equipped with a CCD detector. The data were corrected for Lorentz and polarization effects. Data reduction was performed using *CrysAlis Pro*, Version 1.171.35.21 (Agilent Technologies, 2012), including analytical numeric absorption correction using a multifaceted crystal model based on expressions derived by Clark and Reid (1995). The crystal structure of the mineral was

TABLE 5. Selected interatomic distances (Å) in the structure of melanarsite.

As(1)	–O(1)	1.666(12) × 2	Cu(2)	–O(10)	1.901(12)
As(1)	–O(9)	1.697(12) × 2		–O(1)	1.981(13)
<As(1)–O>		1.68		–O(7)	1.988(11)
				–O(3)	2.040(12)
As(2)	–O(4)	1.664(13) × 2		–O(8)	2.418(12)
	–O(6)	1.706(13) × 2		–O(2)	2.574(12)
<As(2)–O>		1.68	<Cu(2)–O>		2.15
As(3)	–O(5)	1.682(13)	Cu(3)	–O(10)	1.928(11)
	–O(8)	1.683(11)		–O(10)	1.975(11)
	–O(3)	1.687(13)		–O(8)	1.989(11)
	–O(2)	1.688(12)		–O(4)	1.991(13)
<As(3)–O>		1.68		–O(9)	2.485(12)
(Fe,Cu)	–O(7)	1.900(12)		–O(5)	2.706(14)
	–O(10)	1.931(12)	<Cu(3)–O>		2.18
	–O(9)	1.941(11)	K(1)	–O(3)	2.800(13) × 2
	–O(5)	1.983(14)		–O(1)	2.862(14) × 2
	–O(5)	2.354(16)		–O(8)	2.888(11) × 2
	–O(6)	2.400(14)		–O(4)	3.052(15) × 2
<(Fe,Cu)–O>		2.08	<K(1)–O>		2.90
Cu(1)	–O(7)	1.916(12)	K(2)	–O(1)	2.720(13)
	–O(7)	1.929(11)		–O(3)	2.722(13)
	–O(2)	1.958(12)		–O(6)	2.734(14)
	–O(6)	1.995(13)		–O(9)	2.790(12)
	–O(2)	2.401(14)		–O(2)	3.033(14)
	–O(3)	2.777(13)		–O(4)	3.210(17)
<Cu(1)–O>		2.16		–O(4)	3.308(15)
			<K(2)–O>		2.93

TABLE 6. Bond-valence calculations for melanarsite*.

	As(1)	As(2)	As(3)	(Fe,Cu)	Cu(1)	Cu(2)	Cu(3)	K(1)	K(2)	Σ
O(1)	$1.31^{x2\downarrow}$					0.44		$0.14^{x2\downarrow}$	0.20	2.09
O(2)			1.24		0.47	0.09			0.09	2.03
					0.14					
O(3)			1.24		0.05	0.38		$0.16^{x2\downarrow}$	0.20	2.03
O(4)		$1.32^{x2\downarrow}$					0.43	$0.08^{x2\downarrow}$	0.05	1.92
									0.04	
O(5)			1.26	0.49			0.06			1.99
				0.18						
O(6)		$1.18^{x2\downarrow}$		0.16	0.43				0.19	1.96
O(7)				0.62	0.53	0.43				2.09
					0.51					
O(8)			1.25			0.14	0.43	$0.13^{x2\downarrow}$		1.95
O(9)	$1.21^{x2\downarrow}$			0.56			0.11		0.17	2.05
O(10)				0.56		0.55	0.51			2.07
							0.45			
Σ	5.04	5.00	4.99	2.57	2.13	2.03	1.99	1.02	0.94	

*Bond-valence parameters were taken from Brese and O'Keeffe (1991).

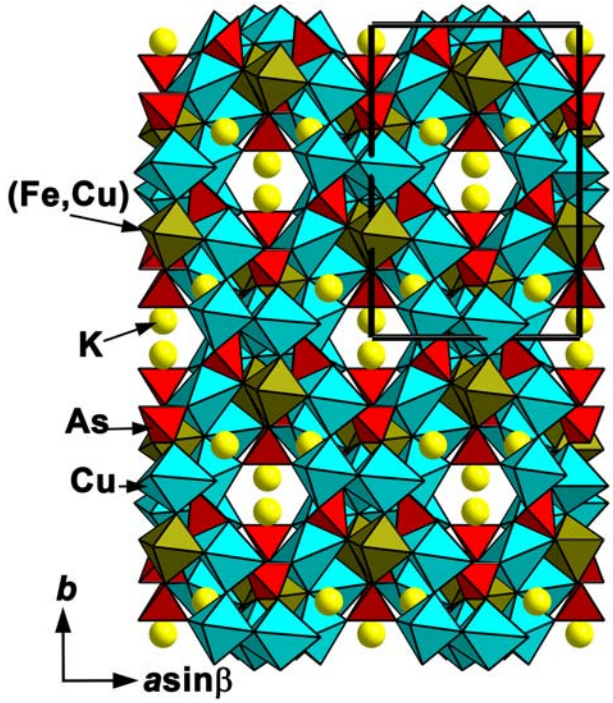

FIG. 7. The crystal structure of melanarsite projected along the *c* axis. The unit cell is outlined.

solved by direct methods and refined with the use of SHELX-97 software package (Sheldrick, 2008) to $R = 0.091$. The unit-cell parameters and the experimental details are presented in Table 3, atom coordinates and displacement parameters in Table 4, selected interatomic distances in Table 5 and bond-valence calculations in Table 6. Even the best of all tested single crystals of melanarsite showed, unfortunately, not very high quality because of a slightly divergent character responsible for the relatively high final value of $R = 9.1\%$. However reasonable values of displacement parameters (Table 3), interatomic distances (Table 4) and bond-valence parameters (Table 5), as well as good agreement between the measured and calculated powder X-ray diffraction data (Table 2) demonstrate that the determined structure is correct.

Discussion

No mineral or synthetic compound close to melanarsite in terms of crystal structure is known. Two recently discovered anhydrous oxyarsenates with species-defining Cu and K, shchurovskyite $K_2CaCu_6O_2(AsO_4)_4$ and dmisokolovite $K_3Cu_5AlO_2(AsO_4)_4$ (Pekov *et al.*, 2015*c*), are related to one another but differ from melanarsite in both stoichiometry and structure. All three of these K-Cu arsenates are closely associated and can be easily distinguished from each other due to their quite different colours (Fig. 1).

The crystal structure of melanarsite (Fig. 7) is based upon the heteropolyhedral pseudo-framework built by distorted Cu(1–3)O_6 and (Fe,Cu)O_6 octahedra and As(1–3)O_4 tetrahedra. All Cu-centred octahedra are characterized by strong Jahn-Teller distortion with four short Cu–O distances in the ranges 1.916(12)–1.995(13) Å [Cu(1)], 1.901(12)–2.040(12) Å [Cu(2)] and 1.928(11)–1.991(13) Å [Cu(3)] and two elongated Cu–O bonds, 2.401(14) and 2.777(13) Å for Cu(1), 2.418(12) and 2.574(12) Å for Cu(2), and 2.485 (12) and 2.706(14) Å for Cu(3). The (Fe,Cu)O_6 octahedron, occupied by Fe^{3+} and Cu^{2+} cations as ($Fe_{0.5}Cu_{0.5}$), is also characterized by Jahn-Teller distortion but not as strong; four short (Fe,Cu)–O distances are in the range 1.900(12)–1.983(14) Å whereas two elongated bonds are 2.354(16) and 2.400(14) Å. Cu(1)O_6 octahedra are connected *via* common edges to form zig-zag chains running

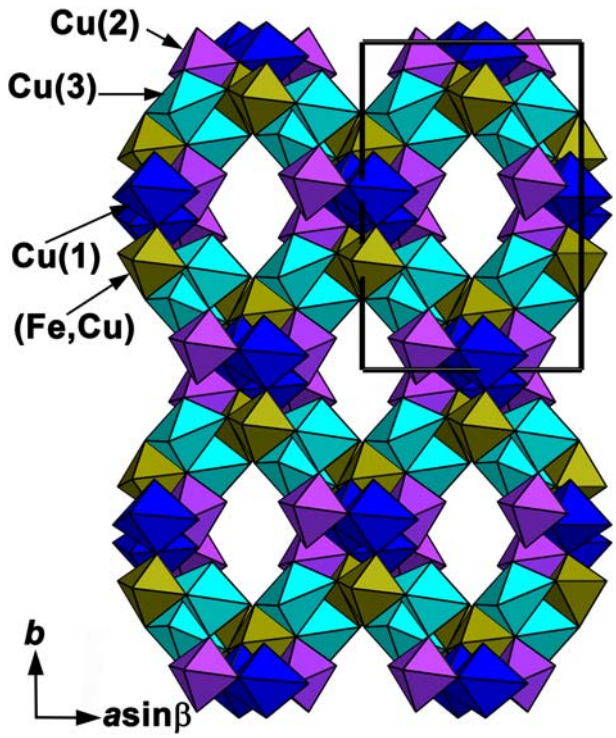

FIG. 8. The motif formed by Cu- and (Fe,Cu)-centred polyhedra in the crystal structure of melanarsite. The unit cell is outlined.

along the *c* axis. The Cu(3)-centred octahedra share common edges forming dimers, as well as the (Fe, Cu)-centred octahedra. The $[Cu(3)_2O_{10}]$ and $[(Fe, Cu)_2O_{10}]$ dimers share common edges building complicated chains connected on two sides by isolated $Cu(2)O_6$ octahedra. These fragments are linked by the chains of Cu(1)-centred octahedra (Fig. 8). For better clarity, octahedra occupied by three crystallographically independent Cu cations are shown in different colours in Fig. 8. Three crystallographically independent As atoms occupy AsO_4 tetrahedra connected with Cu- and (Fe,Cu)-centred octahedra via common O vertices to form a heteropolyhedral pseudo-framework with tunnels running along the *c* axis. Two crystallographically independent K^+ cations, K(1) and K(2), are located in the tunnels and voids of the pseudo-framework centring eight- and seven-fold polyhedra, respectively.

Oxygen atoms O(7) and O(10) in melanarsite are bound only to Cu and (Fe,Cu) and, therefore, the crystal structure of the mineral could be described in terms of anion-centred tetrahedra. The O-centred tetrahedra $OCu_3(Fe,Cu)$ are connected via common Cu(1)–Cu(1), Cu(3)–Cu(3) and Cu(2)–(Fe,Cu) edges to form infinite, isolated chains of composition $[O_4Cu_6(Fe,Cu)_2]^{\infty}$ (Fig. 9). Similar chains were reported in piypite $K_8Cu_9O_4(SO_4)_8Cl_2$ (Effenberger and Zemann, 1984; described as caratiite), its synthetic sodium analogue $Na_4Cu_4O_2(SO_4)_4{\cdot}MeCl$ (M = Na, Cu, □) (Kahlenberg *et al.*, 2000), coparsite $Cu_4O_2[(As, V)O_4]Cl$ (Starova *et al.*, 1998) and recently discovered wulffite $K_3NaCu_4O_2(SO_4)_4$ and parawulffite $K_5Na_3Cu_8O_4(SO_4)_8$ (Pekov *et al.*, 2014*d*).

The crystal chemical formula of melanarsite is $^{K(1)}K^{K(2)}K_2^{Cu(1)}Cu_2^{Cu(2)}Cu_2^{Cu(3)}Cu_2^{(Fe,Cu)}(Fe^{3+}_{0.5}Cu_{0.5})_2O_4(AsO_4)_4$ (Table 3) and corresponds to the idealized formula $K_3Cu_7Fe^{3+}O_4(AsO_4)_4$. The presence of iron in the (Fe,Cu) site as Fe^{3+} is confirmed by bond-valence calculations (Table 5) and the distinctly smaller size of this octahedron in comparison with Cu(1–3)-centred octahedra; average interatomic distances are 2.16, 2.15 and 2.18 Å for the latter

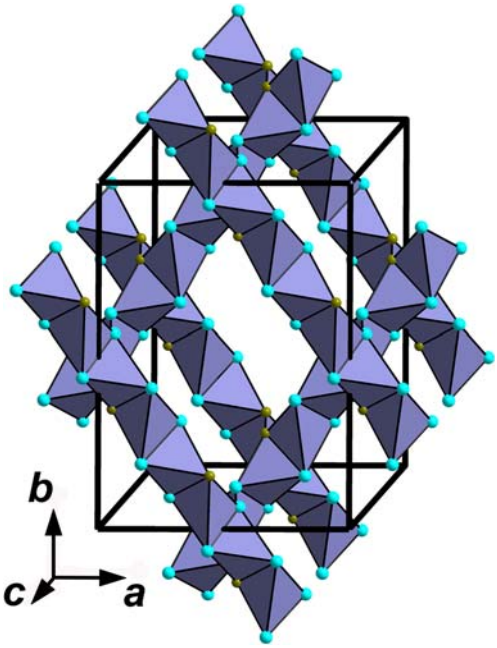

FIG. 9. The chain motif formed by oxocentred tetrahedra $OCu_3(Fe,Cu)$ in melanarsite. Blue circles are Cu(1–3) sites, olive green circles are (Fe,Cu) sites. The unit cell is outlined.

and 2.08 Å for the former (Table 4). The Fe:Cu ratio in this site is close to 1.00, $(Fe^{3+}_{0.5}Cu^{2+}_{0.5})$. A very similar situation was reported for the Cu-rich variety of lyonsite, $Cu_{3+x}(Fe^{3+}_{4-2x}Cu_{2x})(VO_4)_6$, found in the Yadovitaya fumarole at the same Second scoria cone of the Northern Breakthrough of the Great Tolbachik Fissure Eruption; here the (Fe,Cu) site content is $(Fe^{3+}_{0.55}Cu^{2+}_{0.45})$ (Pekov *et al.*, 2013). Significant substitution of Fe^{3+} by Cu^{2+} was reported for another sublimate mineral from the Tolbachik fumaroles, hatertite $Na_2(Ca,Na)(Fe^{3+},Cu)_2(AsO_4)_3$, in which the *M*(2) site contains $(Fe^{3+}_{0.45}Cu^{2+}_{0.20}Al_{0.19}Zn_{0.16})$ (Krivovichev *et al.*, 2013).

The presence of only Fe^{3+} or its strong preference over Fe^{2+} is a typical feature of the sublimate minerals formed in the fumaroles at the Second scoria cone of the Northern Breakthrough of the Great Tolbachik Fissure Eruption, characterized by strongly oxidizing conditions (Vergasova and Filatov, 2012; Pekov *et al.*, 2014*b*). This was obviously caused by the mixing of volcanic gases with the atmospheric air here (Meniaylov *et al.*, 1980; Zelenski *et al.*, 2012). High oxygen fugacity in gases is clearly confirmed by the presence of S, As and Mo only in the forms of sulfate, arsenate and molybdate minerals, respectively, in incrustations of fumaroles at the Second scoria cone of the Northern Breakthrough of the Great Tolbachik Fissure Eruption.

Under reducing conditions, As in volcanic fumaroles is incorporated mainly in different sulfides or in As-bearing amorphous sulfur formed at relatively low temperatures (below 300°C), as both empirical data [e.g. for sulfide-bearing fumaroles at such volcanoes as Vulcano (Aeolian Archipelago, Italy), Satsuma-Iwojima (Kyushu, Japan) and Mutnovsky (Kamchatka, Russia)] and thermodynamic modelling show (Symonds *et al.*, 1987; Symonds and Reed, 1993; Cheynet *et al.*, 2000; Africano *et al.*, 2002; Zelenski and Bortnikova, 2005). However, an increase of oxygen fugacity (as a result of the mixing of volcanic gases with the air) may reduce the volatility of some elements, including As (Africano *et al.*, 2002), and this could increase the temperature of crystallization of arsenic (at the first time, of As^{5+}) phases in a fumarolic system. This assumption is in a good agreement with our temperature measurements in pockets with arsenate minerals in the Arsenatnaya fumarole, 360–380°C for the assemblage with melanarsite and up to 420°C for assemblages with mainly alluaudite-group arsenates and tilasite (measured immediately after the uncovering of pockets). In general, in fumaroles belonging to different types in terms of f_{O_2}, the temperature of formation of arsenic mineralization is different. Arsenates crystallize at significantly higher temperatures than arsenic sulfides and As-containing native sulfur.

Acknowledgements

The authors are grateful to Giovanni Ferraris, Peter Leverett and anonymous referee for valuable comments and Diego Gatta for editorial work. This study was supported by the Russian Science Foundation, grants nos. 14-17-00048 (electron probe, spectroscopic and structure investigations) and 14-17-00071 (powder X-ray diffraction investigation). The technical support by the SPbSU X-Ray Diffraction Resource Center in the PXRD studies is acknowledged.

References

Africano, F., Van Rompaey, G., Bernard, A. and Le Guern, F. (2002) Deposition of trace elements from high temperature gases of Satsuma-Iwojima volcano. *Earth Planets Space*, **54**, 275–286.

Agilent Technologies (2012) *CrysAlisPro* Software system, version 1.171.35.21. Agilent Technologies UK Ltd, Oxford, UK.

Brese, N.E. and O'Keeffe, M. (1991) Bond-valence parameters for solids. *Acta Crystallographica*, **B47**, 192–197.

Cheynet, B., Dall'Aglio, M., Garavelli, A., Grasso, M.F. and Vurro, F. (2000) Trace elements from fumaroles at Vulcano Island (Italy): rates of transport and a thermochemical model. *Journal of Volcanology and Geothermal Research*, **95**, 273–283.

Clark, R.C. and Reid, J.S. (1995) The analytical calculation of absorption in multifaceted crystals. *Acta Crystallographica*, **A51**, 887–897.

Effenberger, H. and Zemann, J. (1984) The crystal structure of caratiite. *Mineralogical Magazine*, **48**, 541–546.

Kahlenberg, V., Piotrowski, A. and Giester, G. (2000) Crystal structure of $Na_4[Cu_4O_2(SO_4)_4]\cdot MeCl$ (Me: Na, Cu, □) – the synthetic Na-analogue of piypite (caratiite). *Mineralogical Magazine*, **64**, 1099–1108.

Krivovichev, S.V., Vergasova, L.P., Filatov, S.K., Rybin, D.S., Britvin, S.N. and Ananiev, V.V. (2013) Hatertite, $Na_2(Ca,Na)(Fe^{3+},Cu)_2(AsO_4)_3$, a new alluaudite-group mineral from Tolbachik fumaroles, Kamchatka peninsula, Russia. *European Journal of Mineralogy*, **25**, 683–691.

Meniaylov, I.A., Nikitina, L.P. and Shapar', V.N. (1980) *Geochemical Features of Exhalations of the Great Tolbachik Fissure Eruption.* Nauka Publishing, Moscow.

Pekov, I.V., Zubkova, N.V., Chernyshov, D.Y., Zelenski, M.E., Yapaskurt, V.O. and Pushcharovsky, D.Y. (2013) A new Cu-rich variety of lyonsite from fumarolic sublimates of the Tolbachik volcano (Kamchatka, Russia) and its crystal structure. *Doklady Earth Sciences*, **448**, 112–116.

Pekov, I.V., Yapaskurt, V.O., Belakovskiy, D.I., Vigasina, M.F., Zubkova, N.V. and Sidorov, E.G. (2014*a*) Pharmazincite, IMA 2014-015. CNMNC Newsletter No. 21, August 2014, page 798; *Mineralogical Magazine*, **78**, 797–804.

Pekov, I.V., Zubkova, N.V., Yapaskurt, V.O., Belakovskiy, D.I., Lykova, I.S., Vigasina, M.F., Sidorov, E.G. and Pushcharovsky, D.Y. (2014*b*) New arsenate minerals from the Arsenatnaya fumarole, Tolbachik volcano, Kamchatka, Russia. I. Yurmarinite, $Na_7(Fe^{3+},Mg,Cu)_4(AsO_4)_6$. *Mineralogical Magazine*, **78**, 905–917.

Pekov, I.V., Zubkova, N.V., Yapaskurt, V.O., Belakovskiy, D.I., Vigasina, M.F., Sidorov, E.G. and Pushcharovsky, D.Y. (2014*c*) New arsenate minerals from the Arsenatnaya fumarole, Tolbachik volcano, Kamchatka, Russia. II. Ericlaxmanite and kozyrevskite, two natural modifications of $Cu_4O(AsO_4)_2$. *Mineralogical Magazine*, **78**, 1527–1543.

Pekov, I.V., Zubkova, N.V., Yapaskurt, V.O., Belakovskiy, D.I., Chukanov, N.V., Lykova, I.S., Savelyev, D.P., Sidorov, E.G. and Pushcharovsky, D.Y. (2014*d*) Wulffite, $K_3NaCu_4O_2(SO_4)_4$, and parawulffite, $K_5Na_3Cu_8O_4(SO_4)_8$, two new minerals from fumarole sublimates of the Tolbachik volcano, Kamchatka, Russia. *The Canadian Mineralogist*, **52**, 699–716.

Pekov, I.V., Zubkova, N.V., Yapaskurt, V.O., Polekhovsky, Y.S., Vigasina, M.F., Belakovskiy, D.I., Britvin, S.N., Sidorov, E.G. and Pushcharovsky, D.Y. (2014*e*) Melanarsite, IMA 2014-048. CNMNC Newsletter No. 22, October 2014, page 1244; *Mineralogical Magazine*, **78**, 1241–1248.

Pekov, I.V., Britvin, S.N., Yapaskurt, V.O., Polekhovsky, Y.S., Krivovichev, S.V., Vigasina, M.F. and Sidorov, E. G. (2015*a*) Arsmirandite, IMA 2014-081. CNMNC Newsletter No. 23, February 2015, page 57; *Mineralogical Magazine*, **79**, 51–58.

Pekov, I.V., Zubkova, N.V., Yapaskurt, V.O., Belakovskiy, D.I., Vigasina, M.F., Sidorov, E.G. and Pushcharovsky, D.Y. (2015*b*) New arsenate minerals from the Arsenatnaya fumarole, Tolbachik volcano, Kamchatka, Russia. III. Popovite, $Cu_5O_2(AsO_4)_2$. *Mineralogical Magazine*, **79**, 133–143.

Pekov, I.V., Zubkova, N.V., Belakovskiy, D.I., Yapaskurt, V.O., Vigasina, M.F., Sidorov, E.G. and Pushcharovsky, D.Y. (2015*c*) New arsenate minerals from the Arsenatnaya fumarole, Tolbachik volcano, Kamchatka, Russia. IV. Shchurovskyite, $K_2CaCu_6O_2(AsO_4)_4$, and dmisokolovite, $K_3Cu_5AlO_2(AsO_4)_4$. *Mineralogical Magazine*, **79**, 1737–1753.

Pekov, I.V., Zubkova, N.V., Belakovskiy, D.I., Yapaskurt, V.O., Vigasina, M.F., Sidorov, E.G. and Pushcharovsky, D.Y. (2016) New arsenate minerals from the Arsenatnaya fumarole, Tolbachik volcano, Kamchatka, Russia. V. Katiarsite, $KTiO(AsO_4)$. *Mineralogical Magazine*, **80**, 639–646.

Sheldrick, G.M. (2008) A short history of *SHELX*. *Acta Crystallographica*, **A64**, 112–122.

Starova, G.L., Krivovichev, S.V. and Filatov, S.K. (1998) Crystal chemistry of inorganic compounds based on chains of oxocentered tetrahedra. II. The crystal structure of $Cu_4O_2[(As,V)O_4]Cl$. *Zeitschrift für Kristallographie*, **213**, 650–653.

Symonds, R.B. and Reed, M.H. (1993) Calculation of multicomponent chemical equilibria in gas-solid-liquid systems: calculation methods, thermochemical data, and applications to studies of high-temperature volcanic gases with examples from Mount St. Helens. *American Journal of Science*, **293**, 758–864.

Symonds, R.B., Rose, W.I., Reed, M.H., Lichte, F.E. and Finnegan, D.L. (1987) Volatilization, transport and sublimation of metallic and non-metallic elements in high temperature gases of Merapi Volcano, Indonesia. *Geochimica et Cosmochimica Acta*, **51**, 2083–2101.

Vergasova, L.P. and Filatov, S.K. (2012) New mineral species in products of fumarole activity of the Great

Tolbachik Fissure Eruption. *Journal of Volcanology and Seismology*, **6**, 281–289.

Zelenski, M. and Bortnikova, S. (2005) Sublimate speciation at Mutnovsky volcano, Kamchatka. *European Journal of Mineralogy*, **17**, 107–118.

Zelenski, M.E., Zubkova, N.V., Pekov, I.V., Polekhovsky, Yu. S. and Pushcharovsky, D.Yu. (2012) Cupromolybdite, $Cu_3O(MoO_4)_2$, a new fumarolic mineral from the Tolbachik volcano, Kamchatka Peninsula, Russia. *European Journal of Mineralogy*, **24**, 749–757.